



Article

# Modeling and Dynamic Simulation of an Integrated Agrivoltaic-Hydrogen System for the Energy Saving of an Agro-Industrial User

Maria Vicidomini

Department of Industrial Engineering, University of Naples Federico II, 80125 Napoli, Italy; maria.vicidomini@unina.it

**How To Cite:** Vicidomini, M. Modeling and Dynamic Simulation of an Integrated Agrivoltaic-Hydrogen System for the Energy Saving of an Agro-Industrial User. *Materials and Sustainability* 2026, 2(2), 5. <https://doi.org/10.53941/matsus.2026.100005>

Received: 6 June 2025

Revised: 22 January 2026

Accepted: 18 March 2026

Published: 2 May 2026

**Abstract:** This work aims at modeling and simulating an integrated agrivoltaic-hydrogen energy system designed to meet the electricity needs of an agro-industrial user. Specifically, the system integrates an agrivoltaic plant with a green hydrogen storage system, which includes the production of the energy carrier via alkaline electrolysis. A hydrogen storage system based on pressurized tanks, as well as a proton exchange membrane fuel cell (PEMFC) to generate electricity were included in the renewable plant. The modelling and simulation of the system were carried out using the TRNSYS18 software, in order to evaluate the energy and economic performance of the proposed plant and comparing it with the reference system. After the detailed evaluation of the electricity demand of the considered agro-industrial user, i.e., a cheese factory located at Naples (South of Italy), the proposed plant was suitably designed, highlighting the results in terms of energy, economic, and environmental performance. The study also includes a detailed sensitivity analysis in order to consider the variation of the incentives on the economic feasibility of the investigated plant. The proposed system achieves a primary energy ratio of 64%. Moreover, it allows the electric energy withdrawn from the grid to be reduced to only 42% of the total electric energy demand. As a result, the system enables an annual economic saving of about 65,000 €. The results obtained provide a clear overview of the technical and economic feasibility of integrating an agrivoltaic-hydrogen system in the agro-industrial sector, highlighting its potential for a concrete and sustainable energy transition.

**Keywords:** agrivoltaic-hydrogen system; thermoeconomic analysis; dynamic simulation; biocircular economy

## 1. Introduction

The growing awareness of the environmental impact associated with the use of fossil fuels, along with ambitious energy transition policies, is driving the development of renewable energy sources to reduce CO<sub>2</sub> emissions and combat climate change. The European Union, in line with the goals of the 2030 Agenda, has set the target of carbon neutrality by 2050, promoting strategies to improve energy efficiency and encourage sustainable solutions for energy production and use. In this context, the integration of renewable and innovative energy systems represents a crucial step for a sustainable transition and the achievement of energy independence [1]. In this framework, Europe, one of the continents most engaged in environmental issues, needs policies to promote and support technologies that use hydrogen as an alternative fuel that limits dependence on fossil fuels, to make progress in the adoption of an Economy of Hydrogen [2]. The hydrogen applications contribute to decarbonize different sectors [3,4], guaranteeing an effective process with flexibility and high efficiency [5] and serving as long-term energy storage [6]. The use of hydrogen coupled with renewable energy sources is a potential way to



**Copyright:** © 2026 by the authors. This is an open access article under the terms and conditions of the Creative Commons Attribution (CC BY) license (<https://creativecommons.org/licenses/by/4.0/>).

**Publisher's Note:** Scilight stays neutral with regard to jurisdictional claims in published maps and institutional affiliations.

the development of smart energy networks for electrified and hydrogen cities [7]. For longer storage applications (months or weeks) long-term electricity storage, based on hydrogen tend become more effective than batteries considering their efficiency decreasing and increasing capital cost proportionally with the storage capacity [8,9]. With the coupling of solar [10,11] and/or wind technologies [12,13], the renewable power excesses [13] are exploited by electrolyser for the water conversion into hydrogen, which is then stored in metal hydrides or pressurized cylinders, in order to be re-electrified by fuel cells, in periods of renewable energy shortage. The efficiency of H<sub>2</sub> systems is not affected by the storage periods, and more importantly, the size of their main cost elements (i.e., of the electrolyzer and the fuel cell) is determined by the magnitude of the power surpluses and shortages, so their overall cost is only slightly affected by the storage capacity [14].

In this paper, this paradigm was implemented for the decarbonization of an agro-industrial user. The agro-industrial sector plays a key role in the Italian economy, both in terms of energy consumption and environmental impact. Italy is one of the world's leading producers of cheese and other dairy products, with an energy-intensive supply chain that spans from milk processing to refrigeration, packaging, and distribution. This sector is characterized by significant and continuous thermal and electrical energy demands, often met through conventional fossil-based systems, which contribute to greenhouse gas emissions. The integration of renewable energy and hydrogen-based technologies into agro-industrial processes offers a promising pathway to improve sustainability, reduce operational costs, and enhance energy self-sufficiency. In particular, the decarbonization of dairy production aligns with broader national and European climate targets, while also supporting rural development and energy resilience in agricultural areas. The proposed layout represents an ideal opportunity for the limitation of fossil fuels used by a renewable and hydrogen technologies. In particular, the renewable source coupled with the hydrogen production unit is based on an agrivoltaic solar field. In this context, the proposed arrangement allows for the enhancement of agricultural land through the simultaneous integration of energy and agricultural production, optimizing resource use and contributing to greater sustainability and energy self-sufficiency. Specifically, the system integrates an agrivoltaic plant with a green hydrogen storage system, which includes the production of the energy carrier via alkaline electrolysis. A hydrogen storage system based on pressurized tanks, as well as a proton exchange membrane fuel cell (PEMFC) to generate electricity were included in the renewable plant. The whole plant was simulated in TRNSYS environment and suitable energy, economic and environmental analyses were performed in order to assess the proposed integrated agrivoltaic-hydrogen system.

### *Novelty of the Work*

This study presents a novel application of an integrated agrivoltaic-hydrogen energy system tailored to the specific needs of an agro-industrial user, with a focus on the dairy sector. Unlike previous works that often address hydrogen integration at large scale or in generic contexts, this paper introduces a site-specific energy model that combines photovoltaic agricultural land use (agrivoltaics) with hydrogen production via alkaline electrolysis, pressurized storage, and energy recovery through PEM fuel cells. The originality lies in the coupling of these technologies within a real case study—an operating cheese factory in Southern Italy—using detailed dynamic simulations performed in TRNSYS18. The proposed system is evaluated not only for its energy performance but also through a comprehensive thermo-economic analysis, incorporating national incentive schemes and sensitivity analysis on investment subsidies. The work contributes a replicable framework for improving energy self-sufficiency and reducing emissions in energy-intensive agro-industrial supply chains, highlighting a pathway toward practical, scalable, and sustainable decarbonization.

## **2. System Layout**

Figure 1 displays the proposed layout designed for balancing the energy demand of the selected user. The main components of the new energy system are (Figure 1): (i) Agrivoltaic system, (ii) Alkaline electrolyzer, (iii) Intercooled compressor, (iv) Pressurized storage tank, (v) PEM fuel cell. The integrated agrivoltaic-hydrogen system enables the agro-industrial user to maximize energy independence by harnessing solar energy for hydrogen production and storage. Electricity is generated by an agrivoltaic plant, which combines photovoltaic power generation with agricultural use of the underlying land. When production exceeds demand, the surplus energy is either fed into the grid or used to power an electrolyzer that splits water into hydrogen and oxygen. The produced hydrogen is stored in a tank and later used in a PEMFC fuel cell, which converts it back into electricity during periods of low solar irradiation. This system optimizes the use of renewable energy, reduces dependence on the power grid, and enhances the sustainability of the agro-industrial operation. A detail control strategy was implemented in order to manage correctly and efficiently the energy flows of the agrivoltaic-hydrogen plant. Specifically, the control strategy handles power surpluses and deficits to maximize self-consumption and minimize

grid withdrawal. It coordinates the electrolyzer for hydrogen production during surplus times and activates the fuel cell when demand exceeds photovoltaic production, ensuring efficient resource use and optimizing the energy balance of the user. The deficit power management allows to guarantee the user demand. In particular, when the agrivoltaic plant production does not meet the user demand, a power deficit occurs. If the fuel cell cannot be activated, the entire deficit is covered by the grid. The activation of the fuel cell depends on the hydrogen tank level ( $P_{levelTK}$ , this represents the ratio between the pressure of pressurized hydrogen storage tank with respect to the maximum pressure of the pressurized hydrogen storage tank). For this reason, a check on the hydrogen tank level is also implemented. If the tank level is sufficient, the fuel cell can be activated. Otherwise, the deficit power requested by the user is withdrawn from the grid. It is important to note that the fuel cell can provide a maximum power equal to the fuel cell rated capacity. If the power deficit is higher than the fuel cell rated capacity, the grid covers the remaining demand (Figure 2).

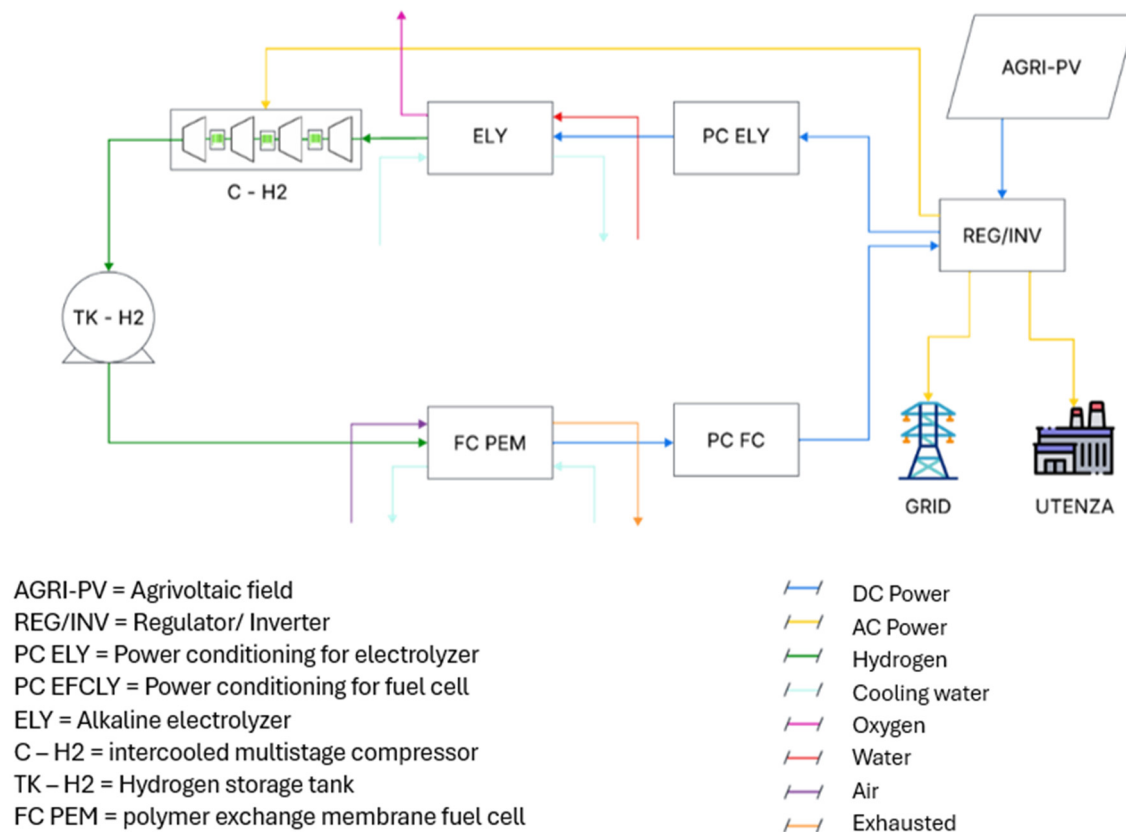


**Figure 1.** System Layout.

Conversely, when agrivoltaic production exceeds the user demand, an energy surplus occurs. This surplus is entirely delivered to the grid if it is not sufficient to activate the electrolyzer. The surplus can be converted into hydrogen, depending on the tank level. If the tank is nearly full, the surplus is delivered to the grid. For the surplus power management, a check is performed in order to compare the surplus with the minimum operating threshold of the electrolyzer. If the surplus is insufficient, it is delivered to the grid. Otherwise, the hydrogen tank level is checked. If the level is lower than 0.90, the surplus can be converted into hydrogen. If the tank is nearly full, the surplus is sent to the grid. If the surplus exceeds the nominal capacity of the electrolyzer, the electrolyzer operates at rated condition, and the excess is delivered to the grid. Otherwise, the entire surplus is used for hydrogen production.

The flowchart representing the operation control strategy for the power deficit and surplus are reported in Figures 2 and 3.

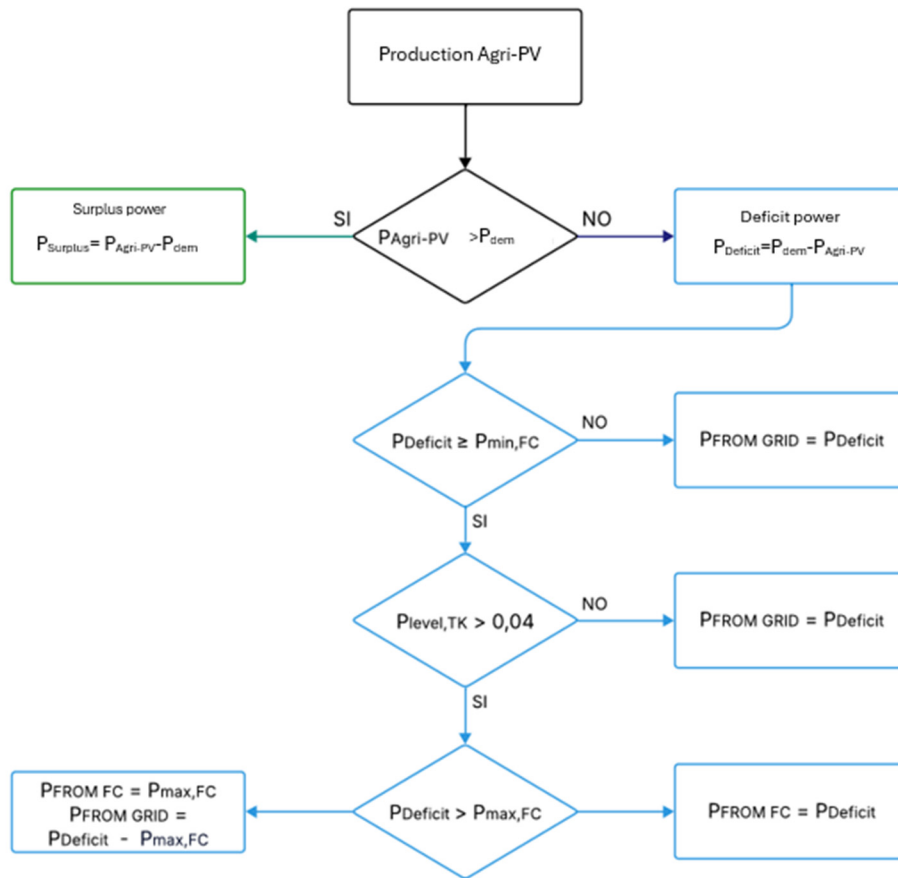


Figure 2. Deficit power control strategy.

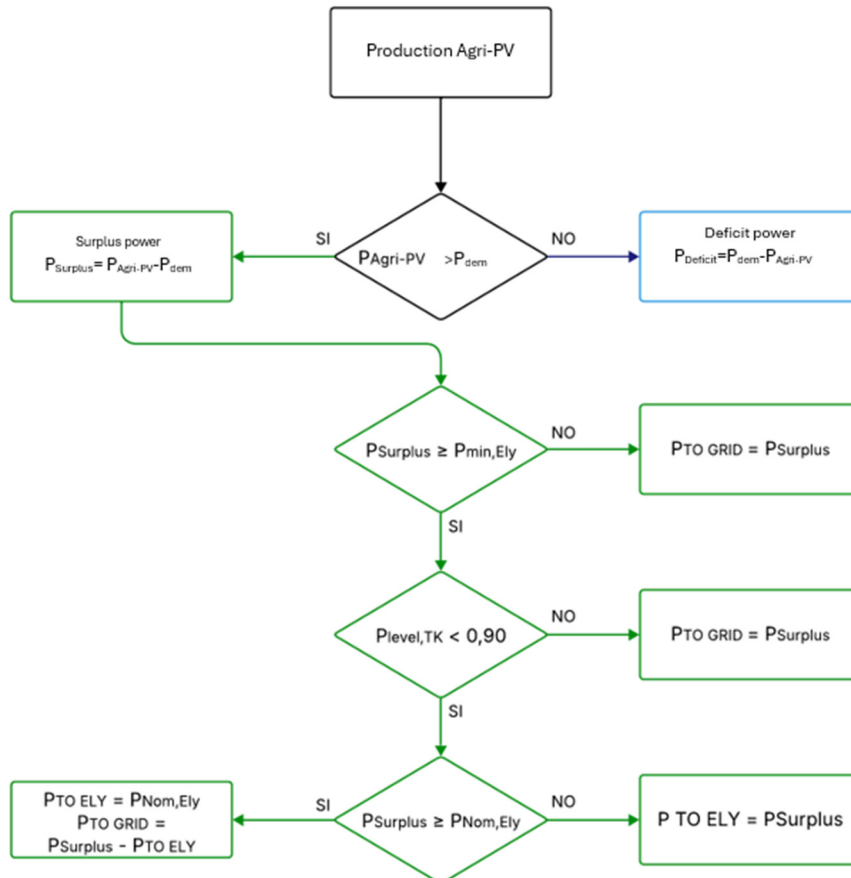


Figure 3. Surplus power control strategy.

Note that the control strategy was designed with the aim of reducing excessive cycling, for example by activating the electrolyzer only when the PV surplus exceeds its minimum operating threshold, and by ensuring that the fuel cell operates primarily during well-defined periods of energy deficit, once a sufficient hydrogen level is reached. A more detailed assessment of component durability, considering cycling-induced degradation, would further strengthen the analysis. In fact, the potential lifetime reduction of the electrolyzer and the fuel cell due to frequent start-up and shutdown cycles is a relevant concern when assessing the long-term reliability and economic viability of hydrogen-based systems. In the present study the primary focus was on evaluating the energy, economic, and environmental performance of the proposed agrivoltaics-hydrogen system. While the dynamic simulation captures the operational behavior of the electrolyzer and fuel cell in response to fluctuating PV production and user demand, it does not explicitly account for degradation effects caused by multiple on-off cycles. This aspect will be investigated in the next studies.

### 3. System Model

The dynamic simulation model of the plant is developed in TRNSYS18 environment. TRNSYS is a reliable and well-known software, commonly used in commercial and academic applications [15]. Note that TRNSYS18 allows the user to adopt in-house and user-developed models [16], but includes a large library of components experimentally validated. The following main TRNSYS libraries are employed in this work:

Type 94 that is able to simulate the PV panel performance, adopting the so-called “four parameters” model. A detailed description is available in Ref. [17]. In particular, this model evaluates the four parameters, characterizing the PV performance, from the manufacture data, in order to evaluate the PV IV-curve for each time step.

Type 175 represents a *Power Conditioning Unit*, capable of operating both as a DC/DC converter and as an inverter (DC/AC and AC/DC). It is based on empirically derived efficiency curves and is specifically optimized for stand-alone electrical systems. It plays a fundamental role in accurately determining the amount of usable energy within hybrid energy systems that integrate PV power generation with hydrogen production via electrolysis, where precise energy management and voltage adaptation are essential for optimal performance and efficiency.

Type 167 simulates the behaviour of a multistage polytropic compressor with intercooling, by calculating the power required for compression. The model allows for one to five compression stages. The model is based on the law of ideal gases in a quasi-static compression process, considering thermodynamic equilibrium for where all stages.

Type 164a represents a high-pressure gas storage tank. To calculate the gas pressure inside the tank, the ideal gas law was considered. The main control parameter is the “pressure level”, which is the ratio between the internal pressure and the maximum permissible pressure.

Type 160 is a high-pressure alkaline water electrolyser, based on principles of fundamental thermodynamics, heat transfer theory and empirical electrochemical relationships. It integrates a dynamic thermal model for the simulation of the behaviour of the electrolyser. The electrochemical approach of the model is based on: (i) an empirical, temperature-dependent (current-voltage) curve specific to a given pressure. (ii) A Faraday efficiency correlation, independent of temperature and pressure.

Type 170 simulates a generic proton exchange membrane (PEM) fuel cell. The overvoltage that contributes to the determination of the polarization curve have been derived empirically.

Note that the considered simulation models consider the part-load behavior and efficiency variations and are able to represent accurately the system’s real performance under varying operating conditions. For example, alkaline electrolyzer and PEM fuel cell (Type 160 and Type 170) do not assume constant efficiency; rather, they simulate performance based on empirical and thermodynamic relationships that vary with load conditions. Specifically, the electrolyzer model includes a temperature-dependent voltage-current curve and a Faraday efficiency correlation, while the fuel cell model accounts for load-dependent overvoltages affecting the polarization curve. As a result, both devices exhibit efficiency values that naturally decrease when operating far from their nominal conditions.

#### *Thermo-Economic Model*

In order to evaluate the energy and economic performance of the proposed renewable plant specific economic and energy performance indices were calculated. The reference energy system is based on a 90 kW photovoltaic plant designed to meet the user electricity demand, considering the grid electric energy integration during hours when solar production is insufficient. The proposed system involves expanding the existing photovoltaic system as an agrivoltaic system coupled with a hydrogen production and utilization system, consisting of an alkaline electrolyzer, a compressor, a pressurized hydrogen storage tank, and a PEM fuel cell. Both systems were compared from the energy point of view by the primary energy saving (*PES*) index. For the economic analysis, incentives

provided by the Italian regulation for agrivoltaic systems, along with a feed-in tariff for net electricity delivered to the grid were considered. The incentive on agrivoltaic systems offering a capital contribution of up to 40% of capital cost, while the feed-in tariff for net electricity delivered to the grid is equal to 0.085 €/kWh. The operating costs of the plant  $C_{PS}$  are evaluated according to the following equation:

$$C_{PS} = EE_{fromGrid} Cu_{EE} - EE_{toGrid} P_{selling,EE} + C_M$$

where  $Cu_{EE}$  is the unit cost for the electric energy withdrawn from the grid, equal to 0.23 €/kWh, according to the user data and  $P_{selling,EE}$  is the unit selling price for the electric energy delivered to the grid. A maintenance cost  $C_M$  equal to 1.5% of the total capital cost was considered. The total capital cost considers the sum of capital costs of the included components, according to the equations reported in Table 1. Here, the specific capital costs adopted for each component are reported.

$$I_{PS} = I_{Agri-PV} + I_{ELY} + I_{FC} + I_{TK} + I_{comp}$$

Both systems were compared from the economic point of view by simple payback period (SPB), net present value (NPV) and profit index (PI), according to the well-known formulas [18]. The economic analysis is performed considering an annuity factor of 12.46 years and a time horizon of the technologies of 20 years.

**Table 1.** Capital costs for economic analysis.

Parameter	Description	Value
$I_{0,PV}$	PV unit capital cost per kW <sub>peak</sub>	1000 [19]
$I_{0,Agri-PV}$	Agrivoltaic unit capital cost	$I_{0,PV} - 0.4 * I_{0,PV} = 600 \text{ €/kW}$
$I_{0,ELY}$	Electrolyzer unit capital cost	1500 €/kW
$I_{0,FC}$	Fuel cell PEM unit capital cost	2000 €/kW
$I_{0,TANK}$	Hydrogen storage tank unit capital cost	500 €/kg
$I_{0,COMP}$	Compressor unit capita cost	$5840 (P_{nom,comp}[kW])^{0.82} \text{ €}$

#### 4. Case Study

The analyzed system is a dairy farm located in Campania (South Italy). The core business of the system is the production of dairy products; it uses different equipment both for the production itself and the tools sterilization. The user consumes thermal and electric energy but in this work the energy measures considered regard only the optimization and decreasing of the electric energy demand. In the reference configuration the user electricity demand is supplied by the grid and a 90 kW PV solar field. The electric hourly demand of the user for a typical day is reported in the following figure (Figure 4). The power load is assessed by means of measured data provided by the energy distributor. The power load is mainly due to the farm activities and to activate the cooling plant.

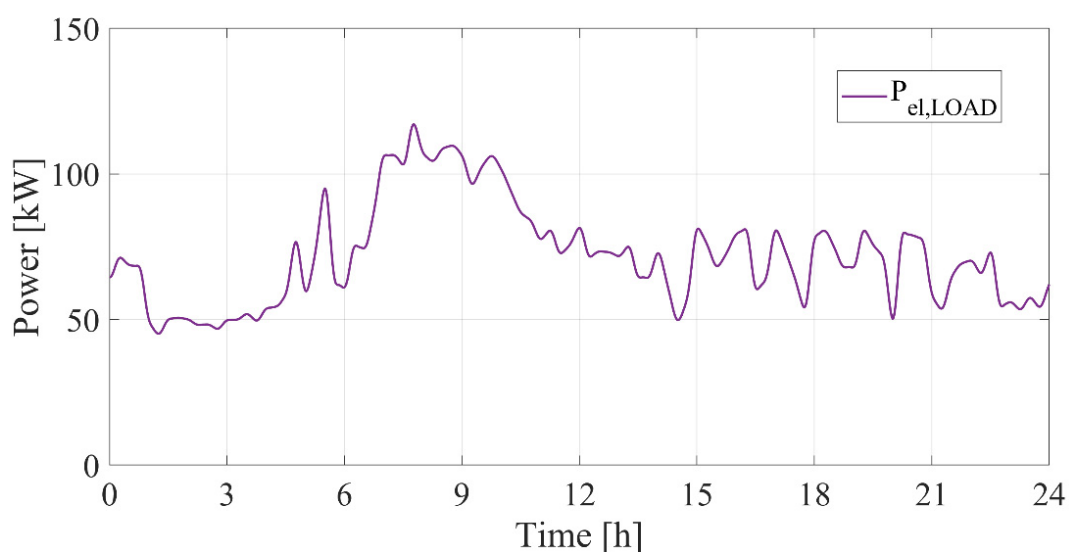


**Figure 4.** Hourly electric load for a typical day.

A significant seasonal trend is detected for the electric load (Figure 5). During the summer months, the electric load increases due to the switching on of the cooling plant.

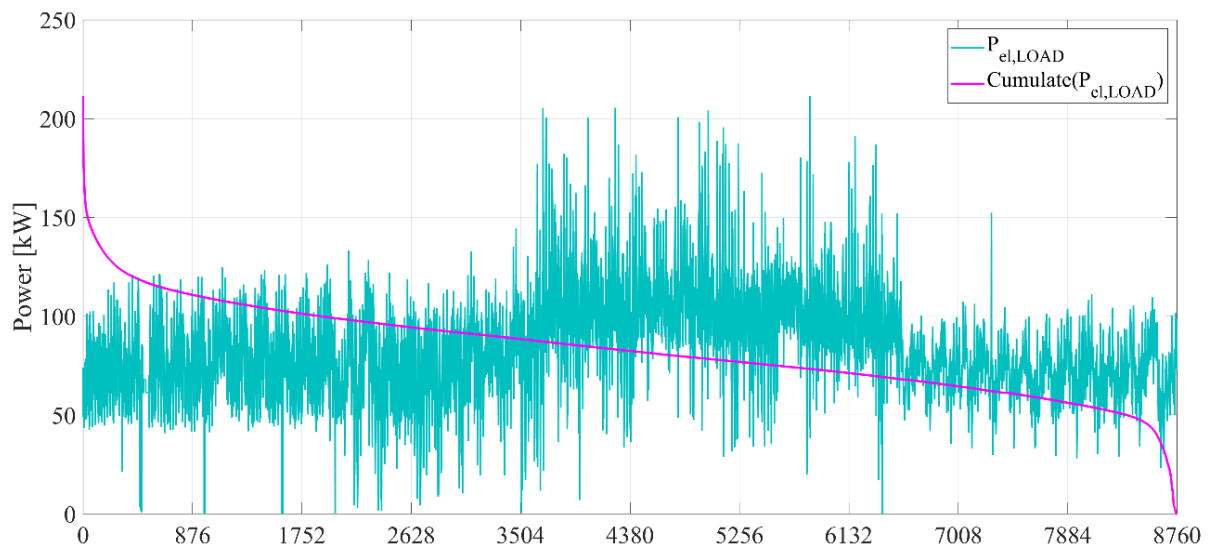


**Figure 5.** Hourly electric load and related cumulated for the whole year.

The yearly electric energy demand is about 775.848 MWh/year. The reference system is supplied by the electricity grid and a 90 kW solar field, producing 148.824 kWh/year that could reduce the energy consumption and costs.

The preliminary sizing of these components was carried out based on:

- The user electricity demand during periods without solar availability;
- The comparison between the user electricity consumption and the photovoltaic plant production.

The proposed system includes the installation of an additional 468 kW agrivoltaic plant, a 300 kW alkaline electrolyzer, a 2 m<sup>3</sup> hydrogen storage tank operating at 250 bar, and a 60 kW PEM fuel cell.

The main data of the components of the proposed and reference systems are reported in Table 2.

**Table 2.** Main components data and features.

Component	Parameter	Description	Value	Unit
<b>PV (reference system)</b>	$\eta_{PV}$	Module efficiency	0.18	-
	$P_{rated,PV}$	PV panel rated power	90	kW
	$A_{tot}$	PV field area	488	m <sup>2</sup>
<b>Agri-PV (proposed system)</b>	$\eta_{PV}$	Module efficiency	0.18	-
	$P_{rated,PV}$	Agri-PV panels rated power	558	kW
	$A_{tot}$	PV field area	3460	m <sup>2</sup>
<b>Electrolyzer</b>	$P_{nom, ELY}$	Electrolyzer rated power	300	kW
	$P_{min, ELY}$	Minimum partial load power	60	kW
	$\eta_{ELY}$	Efficiency	0.65	-
	$N_s, ELY$	Number of cells in series	32	-
	$N_{stack, ELY}$	Number of stacks in parallel	5	-
	$T_{ELY}$	Nominal operating temperature	80	°C
	$p_{ELY}$	Operating pressure	7	bar
	$A$	Electrode area	0.25	m <sup>2</sup>
	$J_{max}$	Maximum cell current density	600	mA/cm <sup>2</sup>
<b>H<sub>2</sub> Storage</b>	$V_{TK}$	Volume	2	m <sup>3</sup>
	$P_{TK}$	Pressure	250	bar
	$M_{TK}$	Maximum hydrogen mass	41	kg
	$T_{TK}$	Temperature	25	°C
	$SoC_{min, TK}$	Minimum tank discharge level	4	%
	$SoC_{max, Tk}$	Maximum tank fill level	90	%
<b>Compressor</b>	$P_{compr}$	Power	28	kW
	$N_{stage}$	Number of stages	4	-

Table 2. Cont.

Component	Parameter	Description	Value	Unit
Fuel cell	$P_{nom, FC}$	Fuel cell capacity	60	kW
	$P_{min, FC}$	Minimum partial load power	15	kW
	$\eta_{FC}$	Efficiency	0.42	-
	$N_{s, FC}$	Number of cells in series	45	-
	$N_{stack, FC}$	Number of stacks in parallel	20	-
	$T_{FC}$	Nominal operating temperature	50	°C
	$A_{Electrode, FC}$	Electrode area	232	cm <sup>2</sup>
	$J_{max, FC}$	Max cell current density	700	mA/cm <sup>2</sup>
	$V_{min, FC}$	Minimum cell voltage	0.7	V

## 5. Results

In this section, the results of the dynamic simulations are presented. In particular, Figures 6 and 7 report the main powers for typical days during winter and summer operation. Tables 3 and 4 report the results of the yearly analysis from the energy, economic and environmental point of view. The analysis of the system daily dynamic performance on a typical winter and summer day allows for a detailed characterization of system. In particular, the following power values are considered:

- $P_{PV}$  [kW]—Power generated by the agrivoltaic system, with an installed capacity of 558 kW.
- User Load [kW]—Power demanded by the agro-industrial user.
- $P_{PVtoUser}$  [kW]—Part of the photovoltaic power supplied to the user to meet instantaneous demand.
- $P_{toELY}$  [kW]—Surplus photovoltaic power converted by the electrolysis process.
- $P_{fromFC}$  [kW]—Power produced by the fuel cell to meet user demand when the PV production is lower than demand.
- $P_{PVtoGrid}$  [kW]—Excess photovoltaic power delivered to the grid.
- $P_{fromGrid}$  [kW]—Power withdrawn from the grid to meet the remaining user demand when the combined photovoltaic and fuel cell power is lower than the user demand.

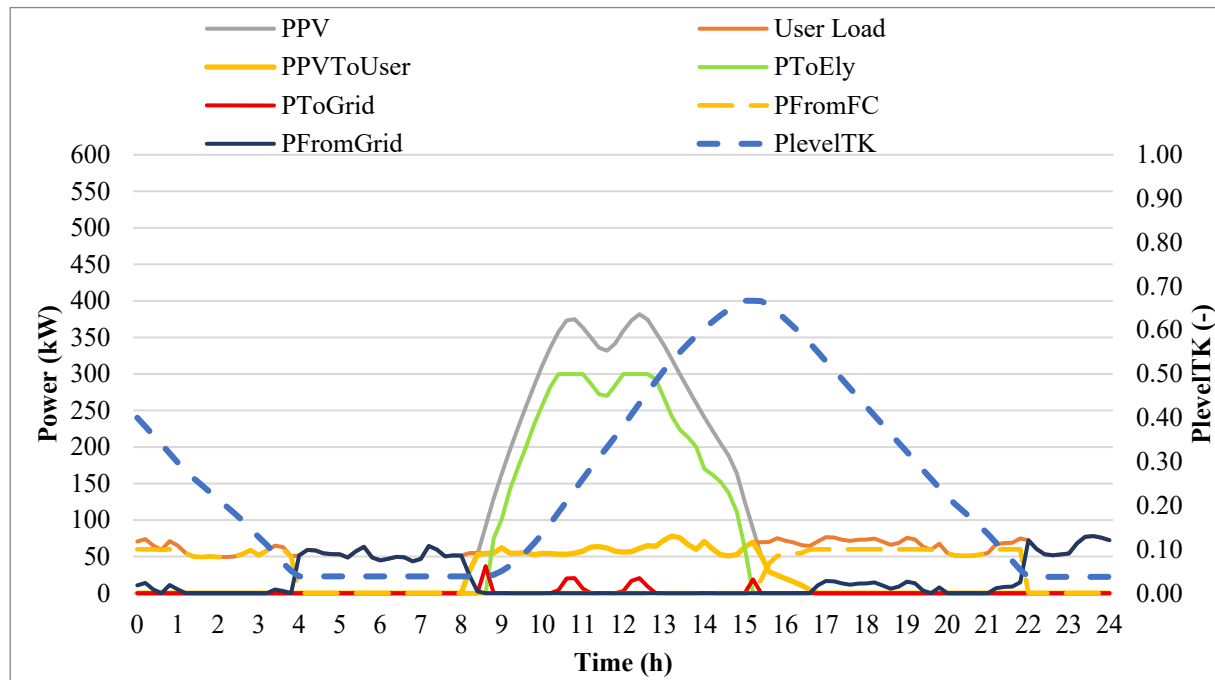


Figure 6. Winter day. Main powers.

Figures 6 and 7 show the 24-h dynamic power profiles for winter and summer days. In both cases, a significant increase in photovoltaic production is observed compared to the user demand, resulting in a substantial power surplus that can be used to power the electrolyzer. Specifically, Figure 6 illustrates the power profiles for a typical winter day. It highlights that, despite photovoltaic production being clearly higher than the production in the reference system (only a 90 kW solar field is considered), it still remains below the nominal capacity of the

plant, reaching a peak of 382 kW at 12:30 PM. It is observed that when the photovoltaic power generated by the agrivoltaic field (PPV) exceeds the user demand (User Load), i.e., between 9:00 AM and 3:00 PM, the energy surplus is primarily used to power the electrolyzer (PtoELY), up to a maximum of 300 kW. Any additional surplus not absorbed by the electrolyzer is fed into the electricity grid (PtoGrid). In this scenario, the power delivered to the grid is limited, while an important amount of the energy is withdrawn from the grid, especially during hours with no photovoltaic production. However, by means the hydrogen storage system, the energy demand met by the grid significantly decreases compared to the reference system. Notably, the fuel cell plays a significant role in meeting user energy demand during the following hours: (i) from 12:00 AM to 4:00 AM, until the hydrogen stored the previous day is depleted, to cover the early morning demand; (ii) from 3:30 PM to 9:30 PM, using the hydrogen produced during the day to cover the evening hours demand. In both cases, the use of the Fuel Cell reduces the use of energy drawn from the grid, improving the energy system self-sufficiency.

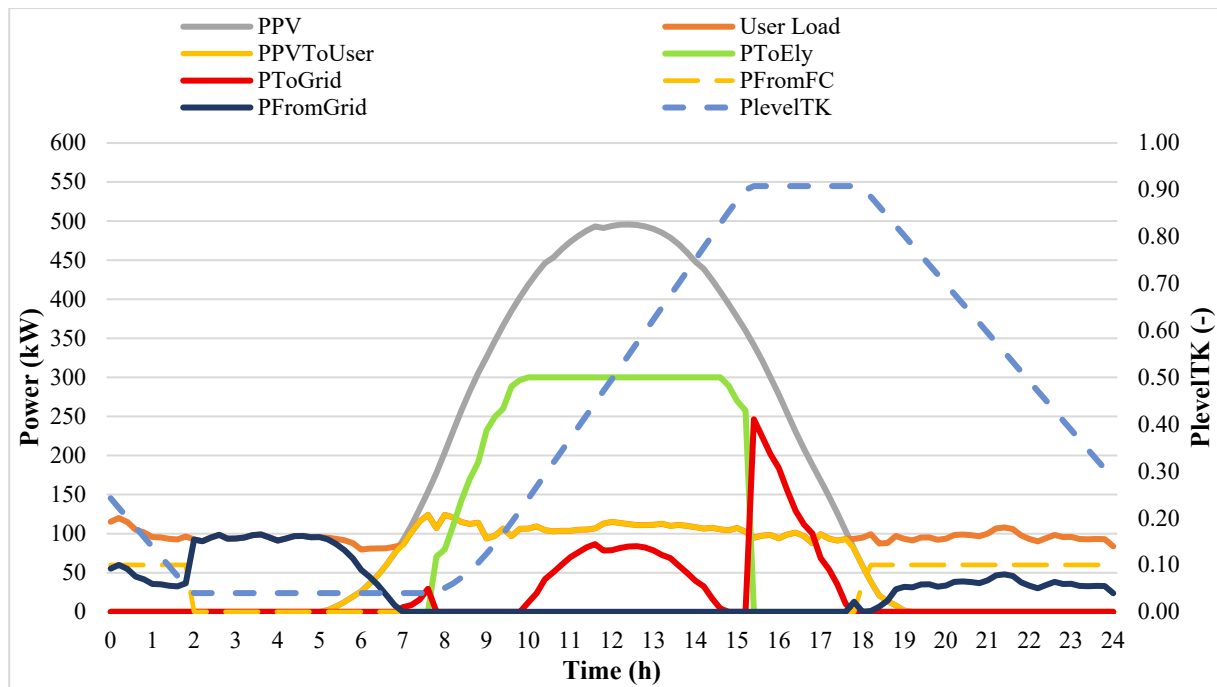


Figure 7. Summer day. Main powers.

Table 3. Yearly energy results.

Parameter	Description	Value	Unit
EE <sub>user</sub>	Electric energy demand of the user	775.8	
EE <sub>user</sub> + EE <sub>compr</sub>	Total electric energy demand (user+compress.)	784.2	
EE <sub>Agri-PV</sub>	PV electric energy production	924.8	
EE <sub>PVtoUtenza</sub>	PV electric energy consumed by the user	331.6	MWh/year
EE <sub>SurplusPV</sub>	PV surplus electric energy	140.6	
EE <sub>comp</sub>	Electric energy consumed by the compressor	8.4	
EE <sub>PVtoELY</sub>	Electricity supplied to the electrolyzer	494.7	
EE <sub>fromFC</sub>	Electricity produced by the fuel cell	126.8	
H2 <sub>prodELY</sub>	Hydrogen production	8.7	t/year
H2 <sub>consFC</sub>	Hydrogen consumption	8.7	t/year
EE <sub>PVtoGrid</sub>	PV electric energy delivered to the grid	98.4	
EE <sub>fromGrid</sub>	Electric energy withdrawn from the grid	325.8	MWh/year
R <sub>Selfconsumed energy (PV + fuel cell)</sub>	Share of user energy demand covered by PV and fuel cell production	58.0	
R <sub>Selfconsumed energy (PV)</sub>	Share of user energy demand covered by PV production	42.0	
EE <sub>fromGrid</sub> /EE <sub>user</sub>	Share of user energy demand covered by the grid	41.5	%
EE <sub>toGrid</sub> /EE <sub>Agri-PV</sub>	Electric energy delivered to the grid	11.0	
EE <sub>toELY</sub> /EE <sub>Agri-PV</sub>	Electric energy supplied to the electrolyzer	53.0	

**Table 4.** Energy, economic and environmental analysis of reference system (RS) and proposed system (PS).

Parameter	Description	Value	Unit
$C_{RS}$	Operating cost RS	146,589	€/year
$C_{PS}$	Operating cost PS	80,986	
$EP_{RS}$	Primary Energy RS	1363	MWh/year
$EP_{PS}$	Primary Energy PS	494.4	
$M_{CO_2,RS}$	CO <sub>2</sub> equivalent emissions RS	303.7	t/year
$M_{CO_2,PS}$	CO <sub>2</sub> equivalent emissions PS	109.2	
$I_{PS}$	Capital cost PS	961,035	€
PES	Primary Energy Saving	868.6	MWh/year
PER	Primary Energy Ratio	64	%
$\Delta C$	Economic saving	65,603	€/year
SPB	Simple Pay Back	14.6	year
DPB	Discounted Pay Back	27.0	
NPV	Net Present Value	−143,480	€
PI	Profit index	−0.15	-

Figure 7 presents the dynamic power profile observed during a typical summer day. In contrast to the winter day previously analyzed, the photovoltaic (PV) generation is considerably higher due to the increased solar irradiance typical of the summer season. Notably, PV power reaches a peak value of 496 kW around 1:00 PM. This generation capacity is sufficient to fully meet the user daytime energy demand, which—as discussed in Case study section—is higher during the summer months. Furthermore, the available power during daylight hours allows the electrolyzer to operate at its nominal capacity between 10:00 AM and 2:30 PM. Within this same interval, a portion of the PV output is delivered to the grid, as the surplus energy—after satisfying the user load—exceeds the electrolyzer rated power. As evidenced in Figure 8, the share of PV power exported to the grid is greater than the the power exported in the winter case, primarily due to two factors:

(i) the increase in PV production resulting from higher summer solar irradiance;

(ii) the saturation of the hydrogen storage tank, which further constrains the system ability to store excess energy. Specifically, around 3:00 PM, although sufficient PV power remains available to continue electrolyzer operation, hydrogen production is stopped as the storage tank reaches its saturation threshold—defined as 90% of its maximum capacity. Consequently, the electrolyzer is deactivated, and the entire energy surplus is delivered to the grid. As for the operation of the fuel cell, its behavior resembles that observed during winter. However, due to the high summer energy demand, the system operates for longer durations at nominal power, thereby necessitating more frequent integration of energy from the grid. In particular, during the summer period, fuel cell operation occurs within the following intervals: from 12:00 AM to 2:30 AM, until the hydrogen stored on the previous day is depleted; from 6:30 PM to 12:00 AM, continuing into the subsequent day until 2:30 AM.

Tables 3 and 4 summarizes the yearly results of the proposed system. A significant improvement in key performance indicators—including operating cost, primary energy consumption, and CO<sub>2</sub> equivalent emissions—can be observed following the implementation of the proposed system. The proposed system is able to reduce the CO<sub>2</sub> equivalent emissions from 303.7 t/year to 109.2 t/year. This is mainly due to the reduction of the electric energy withdrawn from the grid. While the energy results appear promising, the economic indicators reveal values that are notably misaligned with the thresholds typically associated with economically viable investments. At present, hydrogen storage technologies suffer from limited economic competitiveness. Consequently, despite the case study system can benefit from dedicated agrivoltaic incentives, such support proves insufficient to offset the limited financial sustainability of currently available hydrogen storage solutions.

To explore pathways for improving the economic viability of the investment, a sensitivity analysis was conducted focusing on capital grants allocated to the hydrogen storage subsystem. The objective is to identify the incentive value required to enhance the overall economic feasibility of the proposed system. Nonetheless, it is important to contextualize these findings within the current policy framework. Incentives provided under the National Recovery and Resilience Plan (PNRR), predominantly target large-scale industrial plants located in brownfield sites, typically ranging from 1 MW to 10 MW in capacity. This effectively excludes small to medium-scale installations from eligibility. Furthermore, the non-cumulability of incentives imposes an additional constraint: accessing funds for hydrogen production precludes the simultaneous receipt of agrivoltaic incentives, thereby further limiting the financial support available to agro-industrial enterprises. Figure 8 illustrates the behavior of key economic indicators under the scenario in which the agrivoltaic incentive is excluded, and the capital grant for the hydrogen production, storage, and utilization system is varied. The analysis reveals that

increasing the capital support leads to a progressive reduction in both the Simple Payback Period (SPB) and the Discounted Payback Period (DPB), indicating an increasingly shorter investment recovery timeframe. This trend underscores the role of financial incentives in accelerating capital return. Moreover, the Profit Index (PI) exhibits a more-than-linear increase with rising incentives, suggesting that capital grants not only shorten the payback periods but also substantially enhance investment profitability. Notably, the PI only reaches positive values when the capital grant exceeds 55%. At a 60% incentive level, the system records an SPB of 12 years, a DPB of 18 years, and a PI of 5%.

These results confirm that while capital grants for hydrogen storage systems represent a critical lever for improving the economic sustainability of such investments, they are not sufficient, in isolation, to ensure overall profitability. Additional measures or complementary support mechanisms may therefore be necessary to make small- to medium-scale hydrogen-based energy systems financially viable in the current market context.

In parallel, a parametric analysis was conducted on 96 possible configurations, considering 16 different sizes for the agrivoltaic system and 6 for the electrolyzer. From these analyses, the most economically advantageous configurations involve the installation of electrolyzers with a power of 60 kW.

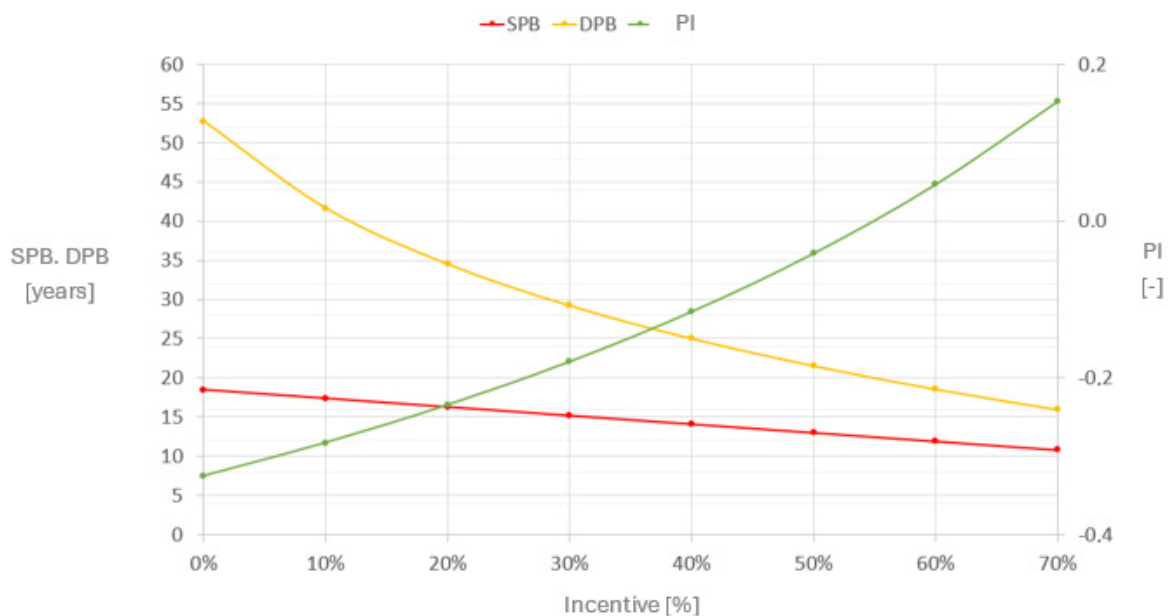


**Figure 8.** Analysis of Economic Indicators as a Function of Incentive Variation for the Hydrogen Plant.

## 6. Conclusions

This paper aimed at developing a dynamic simulation and an economic and environmental analysis of an integrated agrivoltaic-hydrogen energy system. The simulations were carried out using the TRNSYS software, enabling first the dynamic analysis of the reference energy system and subsequently the definition of a solution aimed at maximizing the energy independence of the agro-industrial user. The reference energy system is based on a 90 kW photovoltaic plant designed to meet the user electricity demand, considering the grid electric energy integration during hours when solar production is insufficient. Following a detailed analysis of the load profile and the existing plant production, the adoption of a hydrogen storage system was evaluated. The proposed solution involves expanding the existing photovoltaic system as an agrivoltaic system, by utilizing currently uncultivated land for the cultivation of plant species, functional to the dairy supply chain. This strategy optimizes land use through complementary agricultural production, promotes further gains for the user, and enables access to incentives provided by the Italian regulation for agrivoltaic systems, which offers a capital contribution up to 40% of capital cost, along with a feed-in tariff for net electricity delivered to the grid. The photovoltaic system expansion resulted in increased available power, making it possible to install a hydrogen production and utilization system, consisting of an alkaline electrolyzer, a compressor, a pressurized hydrogen storage tank, and a PEM fuel cell. The following main results can be highlighted:

- Primary energy savings reach 64%, with a corresponding reduction in CO<sub>2</sub> emissions;
- The system can meet the user's electricity demand with a self-consumption rate of 58%;

- The economic analysis indicates a simple payback period (SPB) of 14.6 years, with negative values for the Net Present Value (NPV) and the Profitability Index (PI), assuming a plant lifetime of 20 years.

To improve the economic sustainability of the project, the minimum level of incentive required for the hydrogen system to make the investment financially viable was determined. The analysis showed that, excluding the agrivoltaic incentives (which are not cumulative), the minimum required incentive to ensure non-negative economic results is 60%, highlighting the low competitiveness of the technology. In parallel, a parametric analysis was conducted on 96 possible configurations, considering 16 different sizes for the agrivoltaic system and 6 for the electrolyzer. The results led to a study of how economic indicators vary as a function of the size of the photovoltaic system and the electrolyzer. It emerged that:

- The simple payback period (SPB) is inversely proportional to the agrivoltaic system's power and directly proportional to the electrolyzer power;
- The Net Present Value (NPV) and the Profitability Index (PI) increase with the size of the agrivoltaic plant and decrease as the electrolyzer power increases.

From these analyses, the most economically advantageous configurations involve the installation of electrolyzers with a power of 60 kW. The choice of the agrivoltaic plant size can be more or less constrained by customer requirements (e.g., space availability) or can be optimized based on energy parameters, thus finding a balance between self-consumption and energy fed into the grid.

Note that even if the presented dynamic simulation model captures the operational behavior of the electrolyzer and fuel cell in response to fluctuating PV production and user demand, it does not explicitly account for degradation effects caused by multiple on-off cycles. This aspect will be investigated in the next studies.

## Funding

The author gratefully acknowledges the partial financial support of the project PRIN 2022–AGRIRENEW AGRoIndustrial sector decarbonisation through energy recovery from waste biomass and integration with other RENEWables (CUP: E53D23003030006), funded by the Italian Ministry of University and Research (MUR).

## Data Availability Statement

Author ensures accessibility of data to other competent professionals for at least 10 years after publication

## Conflicts of Interest

The author declares no conflict of interest.

## Use of AI and AI-Assisted Technologies

No AI tools were utilized for this paper.

## References

1. Obiora, S.C.; Olusola, B.; Hu, Y.; et al. Assessing the decarbonization of electricity generation in major emitting countries by 2030 and 2050: Transition to a high share renewable energy mix. *Heliyon* **2024**, *10*, e28770. <https://doi.org/10.1016/j.heliyon.2024.e28770>.
2. Genovese, M.; Schlüter, A.; Scionti, E.; et al. Power-to-hydrogen and hydrogen-to-X energy systems for the industry of the future in Europe. *Int. J. Hydrogen Energy* **2023**, *48*, 16545–16568. <https://doi.org/10.1016/j.ijhydene.2023.01.194>.
3. Incer-Valverde, J.; Patiño-Arévalo, L.J.; Tsatsaronis, G.; et al. Hydrogen-driven Power-to-X: State of the art and multicriteria evaluation of a study case. *Energy Convers. Manag.* **2022**, *266*, 115814. <https://doi.org/10.1016/j.enconman.2022.115814>.
4. Hassan, I.A.; Ramadan, H.S.; Saleh, M.A.; et al. Hydrogen storage technologies for stationary and mobile applications: Review, analysis and perspectives. *Renew. Sustain. Energy Rev.* **2021**, *149*, 111311. <https://doi.org/10.1016/j.rser.2021.111311>.
5. Abdin, Z.; Mérida, W. Hybrid energy systems for off-grid power supply and hydrogen production based on renewable energy: A techno-economic analysis. *Energy Convers. Manag.* **2019**, *196*, 1068–1079. <https://doi.org/10.1016/j.enconman.2019.06.068>.
6. Elmasides, C.; Kosmadakis, I.E.; Athanasiou, C. A comprehensive power management strategy for the effective sizing of a PV hybrid renewable energy system with battery and H<sub>2</sub> storage. *J. Energy Storage* **2025**, *106*, 114790. <https://doi.org/10.1016/j.est.2024.114790>.

7. You, C.; Kim, J. Optimal design and global sensitivity analysis of a 100% renewable energy sources based smart energy network for electrified and hydrogen cities. *Energy Convers. Manag.* **2020**, *223*, 113252. <https://doi.org/10.1016/j.enconman.2020.113252>.
8. Marocco, P.; Ferrero, D.; Gandiglio, M.; et al. A study of the techno-economic feasibility of H<sub>2</sub>-based energy storage systems in remote areas. *Energy Convers. Manag.* **2020**, *211*, 112768. <https://doi.org/10.1016/j.enconman.2020.112768>.
9. Marocco, P.; Ferrero, D.; Lanzini, A.; et al. Optimal design of stand-alone solutions based on RES + hydrogen storage feeding off-grid communities. *Energy Convers. Manag.* **2021**, *238*, 114147. <https://doi.org/10.1016/j.enconman.2021.114147>.
10. Dawood, F.; Shafiullah, G.M.; Anda, M. Stand-Alone Microgrid with 100% Renewable Energy: A Case Study with Hybrid Solar PV-Battery-Hydrogen. *Sustainability* **2020**, *12*, 2047. <https://doi.org/10.3390/su12052047>.
11. Puranen, P.; Kosonen, A.; Ahola, J. Technical feasibility evaluation of a solar PV based off-grid domestic energy system with battery and hydrogen energy storage in northern climates. *Sol. Energy* **2021**, *213*, 246–259. <https://doi.org/10.1016/j.solener.2020.10.089>.
12. Marchenko, O.V.; Solomin, S.V. Modeling of hydrogen and electrical energy storages in wind/PV energy system on the Lake Baikal coast. *Int. J. Hydrogen Energy* **2017**, *42*, 9361–9370. <https://doi.org/10.1016/j.ijhydene.2017.02.076>.
13. Al-Buraiki, A.S.; Al-Sharafi, A. Hydrogen production via using excess electric energy of an off-grid hybrid solar/wind system based on a novel performance indicator. *Energy Convers. Manag.* **2022**, *254*, 115270. <https://doi.org/10.1016/j.enconman.2022.115270>.
14. Marocco, P.; Ferrero, D.; Lanzini, A.; et al. The role of hydrogen in the optimal design of off-grid hybrid renewable energy systems. *J. Energy Storage* **2022**, *46*, 103893. <https://doi.org/10.1016/j.est.2021.103893>.
15. Calise, F. Thermo-economic analysis and optimization of high efficiency solar heating and cooling systems for different Italian school buildings and climates. *Energy Build.* **2010**, *42*, 992–1003. <https://doi.org/10.1016/j.enbuild.2010.01.011>.
16. Klein, S.A.; Mitchell, J.W.; Duffie, J.A.; et al. *Solar Energy Laboratory, TRNSYS; A Transient System Simulation Program*; University of Wisconsin: Madison, WI, USA, 2006.
17. Calise, F.; Cappiello, F.L.; Carteni, A.; et al. A novel paradigm for a sustainable mobility based on electric vehicles, photovoltaic panels and electric energy storage systems: Case studies for Naples and Salerno (Italy). *Renew. Sustain. Energy Rev.* **2019**, *111*, 97–114. <https://doi.org/10.1016/j.rser.2019.05.022>.
18. Cappiello, F.L.; Erhart, T.G. Modular cogeneration for hospitals: A novel control strategy and optimal design. *Energy Convers. Manag.* **2021**, *237*, 114131. <https://doi.org/10.1016/j.enconman.2021.114131>.
19. Buonomano, A.; Calise, F.; d'Accadia, M.D.; et al. A hybrid renewable system based on wind and solar energy coupled with an electrical storage: Dynamic simulation and economic assessment. *Energy* **2018**, *155*, 174–189. <https://doi.org/10.1016/j.energy.2018.05.006>.